World Journal of Advanced Engineering Technology and Sciences

eISSN: 2582-8266

Cross Ref DOI: 10.30574/wjaets

Journal homepage: https://wjaets.com/

(RESEARCH ARTICLE)

Check for updates

Effect of time on alternative hydrocarbon production from waste PS with biodiesel of candlenut oil using catalytic cracking and Si/Al-Ceramic as catalyst

Hendro Juwono *, Arifah Nur Fitriyah, Ita Ulfin and Harmami

Sepuluh November Institute of Technology, Public university in Indonesia.

World Journal of Advanced Engineering Technology and Sciences, 2023, 08(02), 330–338

Publication history: Received on 22 February 2023; revised on 09 April 2023; accepted on 12 April 2023

Article DOI: https://doi.org/10.30574/wjaets.2023.8.2.0103

Abstract

In the present study, the catalytic cracking process of polystyrene (PS) plastic waste and biodiesel of candlenut oil was carried out using Si/Al-ceramic catalyst with a mass ratio of 7:3 at 300 °C. This study aimed to investigate the effect of reaction time on the distribution of hydrocarbon fuel fractions produced. They are characterized by XRD, SEM-EDX, FTIR, and N2 gas adsorption-desorption. The products components of PS catalytic cracking were analyzed by gas chromatography-mass spectroscopy (GC-MS). The liquid fuel obtained was mixed with commercial fuel, Premium RON 88, and methyl tertiary butyl ether (MTBE) additive to determine its physicochemical properties and performance in a generator engine with gasoline-based fuel. The result showed that an increase in reaction time from 60 minutes to 120 minutes of PS cracking over Si/Al-Ceramic catalyst leads to the enrichment of long-chain hydrocarbon fraction (> C12) by 25.61% which is attributed to the formation of styrene dimer. The fuel has thermal efficiency of 26.49% with density of 0.7405 g/cm3, flashpoint of < -50 °C, calorific value of 9642.42 kcal/kg, and octane number of 92.2. These characteristics are in accordance with SNI 06-3506-1994 standard. Therefore, liquid fuel from catalytic cracking of polystyrene plastic wastes can be used as a potential alternative fuel in the gasoline range.

Keywords: Catalytic cracking; Polystyrene; Candlenut oil; Liquid fuel; Si/Al-Ceramic

1. Introduction

Polystyrene (PS) is widely used for some purposes such as packaging, food container, etc. However, this broadly use generates lots of wastes and causes environmental pollution because of their non-biodegradable nature. Since polystyrene has high energy content [1], chemical and thermal degradation of PS are the most probable recycling approach to recover useful products like monomer and fine chemicals from waste plastic [2]. The catalytic cracking of PS is more favorable as it can reduce the overall energy consumption and enhance selectivity [3], [4], [5].

A great variety of solid acidic catalysts such as zeolite, alumina, and silica-alumina at 350°C have been reported to significantly modify the selectivity of PS cracking process since the major products are benzene, ethylbenzene, and cumene [6]. Moreover, reactivity of the catalyst is influenced by Si/Al ratio which determine the amount of acid site. MCM-41, a well-known mesoporous structure, has few acid site but offers an advantage in term of porosity as it pores lie in the mesoporous size [7]. This disadvantage can be handled by metal impregnation on MCM-41 framework [8], [9]. It was reported by [3], [4] that impregnation of Al metal into MCM-41 lead to an increase in the amount of the acid site and this give a potential material to be used as catalyst in a cracking reaction. In the previous study [10], catalytic cracking of Polypropylene (PP) plastic waste have been carried out using modified Al-MCM-41 and produced liquid fuel product at gasoline fraction with yield of 71.89%.

In this present study, we investigated the catalytic cracking process of polystyrene plastic waste over Al-MCM-41-ceramic. The focus of this study will be placed on the effect of reaction time toward the distribution of liquid

* Corresponding author: Hendro Juwono

hydrocarbon products, especially for the production of long chain hydrocarbon fractions (> C_{12}). In addition, the physio-chemical properties of the resulting fuel oil including density, flash point, calorific value, and octane number are investigated and compared with SNI 06-3506-1994 gasoline oil quality and International Standard HIBER11Z Hibernia Petroleum Canada 2016. The performance of PS fuel blend in term of brake thermal efficiency analysis is also performed in gasoline set engine.

2. Material and methods

Polystyrene (PS) foam was used as feedstock in the catalytic cracking process to produce liquid oil. These raw materials were collected from the disposal site in Keputih, Surabaya. PS foam was prepared by cutting it into small pieces and pressed to reduce its large volume. Commercial Al-MCM-41 catalyst was used for these work.

2.1. Preparation of Catalyst

Al-MCM-41 catalysts were initially activated by putting it into oven at 80 °C for an hour. Unused spark plugs were washed, crushed, and sorted into ceramic parts. The activated Al-MCM-41 catalysts were then mixed with the spark plug ceramic powder with a mass ratio of catalyst by ceramic equals to 7:3. Catalyst blend was made into pellets with a diameter and thickness of 1 cm.

2.2. Catalyst Characterization

The acidity of the catalyst was measured by FTIR in which the sample has saturated steam of pyridine absorption. The N_2 adsorption and desorption measurement of the prepared catalyst were measured by Quantachrome Autosorb iQ gas sorption analyzer at 77.35K. Calculation of the surface area was evaluated using Brunauer-Emmet-Teller (BET) method, while pore size distribution was estimated from the branch of the isotherm using Barret-Joyner-Halenda (BJH) method [11].

Scanning Electron Microscopy (SEM) was used to determine the surface morphology of the catalyst. In addition, Energy Dispersive X-Ray (EDX) analysis was associated to investigate the corresponding elements presented in the sample. The crystallinity and thermal stability of the catalyst were investigated by Wide-Angle X-Ray Diffraction (WAXD) and DTA measurements respectively.

2.3. Catalytic Cracking of Polystyrene

Catalytic cracking processes were conducted in a continuous reactor made of stainless steel. It consists of heating chamber, catalytic reforming chamber, cooling chamber, and collecting chamber as shown in Figure 1. In this work, 500 g of the compressed polystyrene foam was fed into heating chamber. A total of 9 mg of the pelleted catalyst was inserted into catalyst tube filled with glass wool. In addition, nitrogen gas was flowed into heating chamber for a minute to remove oxygen gas. The reactor was heated to 300°C and this temperature was maintained for 60 – 120 minutes at atmospheric pressure. The feedstock was converted into vapors, which were condensed into liquid oil after passing through the cooling chamber and collected in the collecting chamber at the bottom.

3. Results and discussion

3.1. Catalyst Characterization

The type of acidic side of the catalyst, the Bronsted and Lewis acidic side, was determined by FTIR spectroscopic analysis with pyridine as a probe molecule. The FTIR-pyridine spectra depicted in Figure 1 shows several peaks including peak at wave number 1548.89 $cm^{-1}$and 1446.66 cm^{-1} which correspond to Bronsted and Lewis acidic side respectively.

Low peaks around 1455 cm^{-1} and high peaks around 1620 cm^{-1} indicated that pyridine was adsorbed in the Lewis acidic side [12]. On the other hand, Aini reported that peaks at wave number 1638 cm^{-1} and 1545 cm^{-1} was the stretching vibration characteristic of pyridinium ion ($C_5H_5NH^+$), in which pyridine binds to protons. The presence of pyridinium stretching peak proved that there were acidic Bronsted hydroxyl collection. The impregnation of Al metal ions into tetrahedral coordinated silica structures of MCM-41 produce Bronsted acidic side [13]. The amount of each acidic side was given in Table 1.

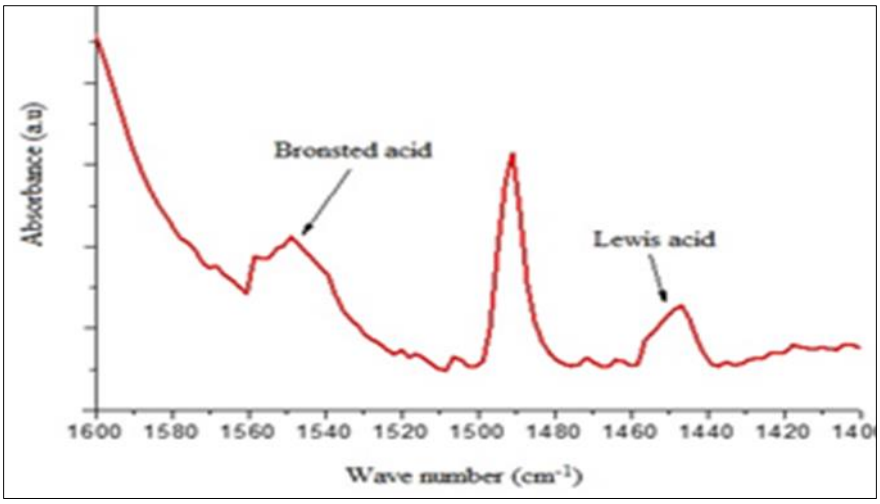

Figure 1 FTIR spectrogram of pyridine adsorption

Table 1 Result of FTIR analysis

Type of acid	Wave number	Amount of acid (mmol/g)
Lewis	1431 – 1460	0.0311
Bronsted	1533 – 1558	0.0342
Total acidic site		0.0653

The result of N_2 adsorption and desorption of the modified catalyst was compared to Al-MCM-41 and given in Figure 2. The graph indicated isotherm type IV which corresponded to a typical graph of Al-MCM-41 catalyst [14]. It revealed that the addition of ceramic with the mass ratio of Al MCM-41: ceramic (7:3) did not change the isotherm graph type of Al-MCM-41. In addition, modification of ceramic into Al-MCM-41 influenced the surface area of catalyst. The result of BET analysis in Table 4 showed that Al-MCM-41-ceramic had larger surface area than Al-MCM-41.

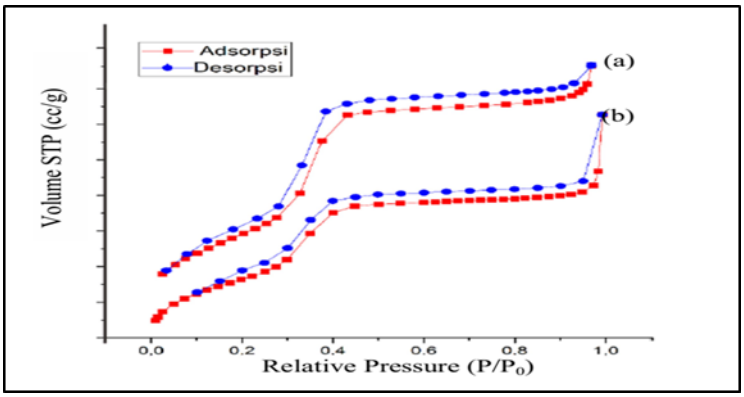

Figure 2 (a) Isotherm graph of Al-MCM-41.(b) Isother m graph of Al-MCM-41-ceramic

The surface area increased by 14.42% as some site in the catalyst surface were occupied by ceramic and the pore volume increased by 8.42%.

Table 2 Result of BET analysis

Catalyst	Surface Area (m^2/g)	Pore Volume (cc/g)
Al-MCM-41	419.93	0.50
Al-MCM-41-ceramic	490.665	0.546

Scanning electron microscopy images showed the morphology of Al-MCM-41 catalyst before and after modification by ceramic. The SEM image of Al-MCM-41 and Al-MCM-41-ceramic were presented in figure 3(a) and 3(b) respectively. In Al-MCM-41, fine surfaces were seen to agglomerate from solids with hexagonal structures, whereas in the Al-MCM-41: ceramic (7: 3) modification, there are fine particles with hexagonal structures attached to the ceramic surfaces that act as solids support [21]. The presence of Al and Si elements in the catalyst is indicated by the red and green colors of the EDX scan results as shown in Figures 4 (a) and 4 (b). Energy Dispersive X-Ray (EDX) analysis provided quantitative information about Si:Al ratio in the corresponding catalyst. Si:Al ratio of Al-MCM-41 catalyst increased from 10 to 14.5 after modification by ceramic since ceramic became the additional source of aluminium. Elemental analysis of Al-MCM-41 and Al-MCM-41-ceramic from EDX were shown in figure 5(a) and 5(b) respectively

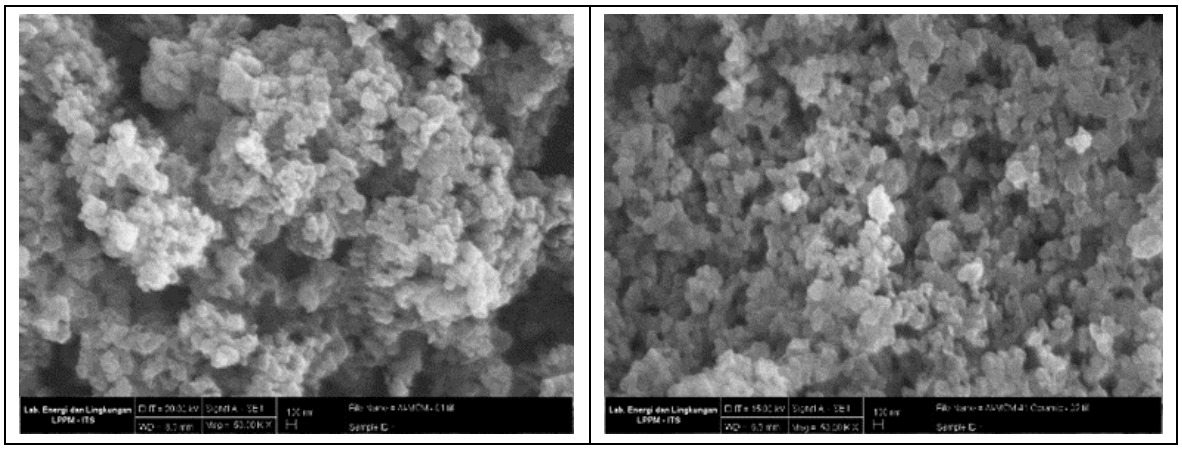

Figure 3 (a). SEM imaging of Al-MCM-41 (b). SEM imaging of Al-MCM-41-ceramic

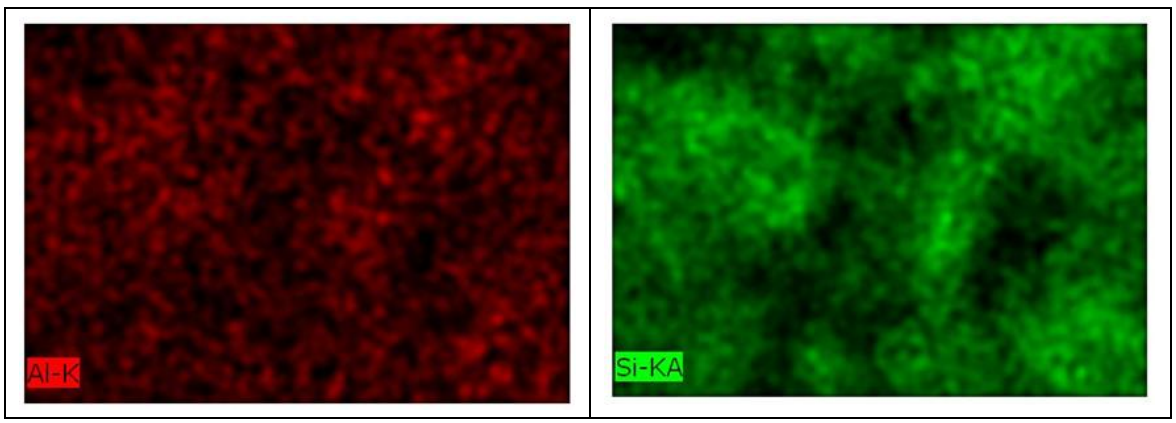

Figure 4 (a). EDX scanning result for metal Al (red) and Si (green) in the Al-MCM-41 catalyst

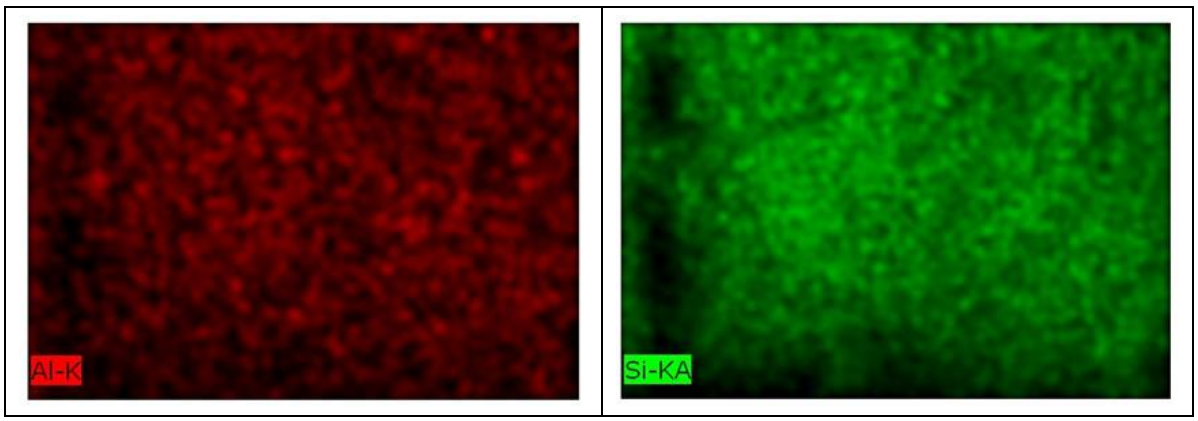

Figure 5 (b). EDX scanning result for metal Al (red) and Si (green) in the Al-MCM-41-ceramic catalyst

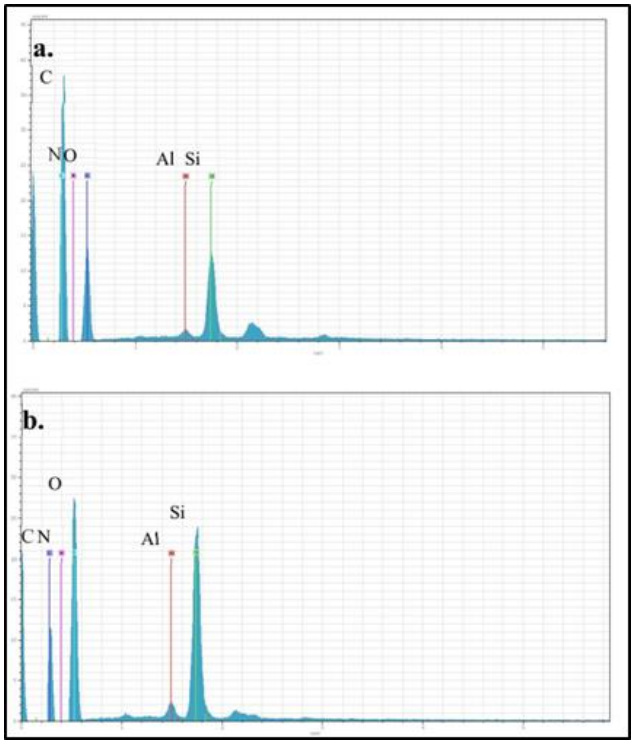

Figure 6 Analysis of elemental abundance from scanning EDX on catalyst (a) Al-MCM-41 (b). Al-MCM-41-ceramic

The diffractogram of Al-MCM-41-ceramic was depicted in Figure 7. Typically, the low angle XRD pattern of the Al-MCM-41 exhibited three well resolved peaks at 2θ = 2.5°, 4.2°, and 4.9° corresponding to the crystalline planes (100), (110), and (200) respectively [15]. After modification of ceramic, the characteristic peaks of the Al-MCM-41 hexagonal structure remained the same, however decreased in its intensity. This decreasing intensity indicated that modification of ceramic did not change the structural properties of Al-MCM-41.

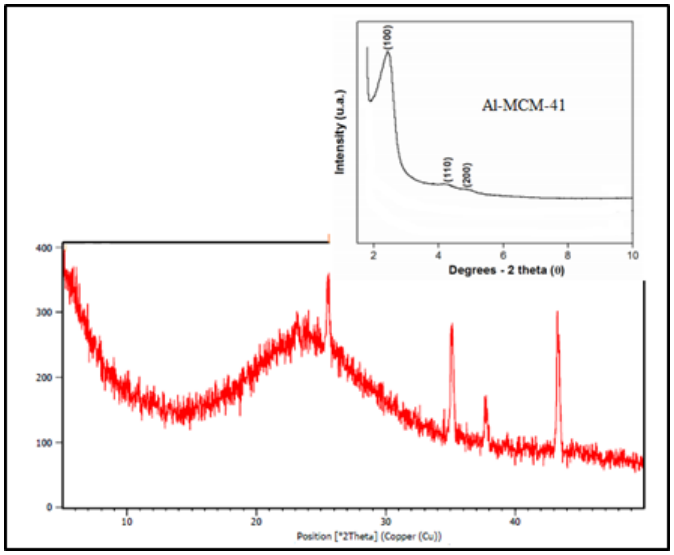

Figure 7 XRD diffractogram of Al-MCM-41-ceramic catalyst

3.2. Catalytic Cracking Process

Catalytic cracking process of PS in the presence of Al-MCM-41-ceramic catalyst was examined at 300 °C under N_2 gas. This observation was conducted for 60 minutes and 120 minutes to investigate the effect of reaction time toward the production of hydrocarbon liquid fraction. PS thermal cracking was also conducted under the same condition for

comparison. The chromatogram of the catalytic cracking products for 60 minutes and 120 minute reaction time were presented successively in Figure 8 (a) and (b), while for PS thermal cracking in (c).

PS catalytic cracking over Al-MCM-41-ceramic in 60 minutes reaction time yielded 0.13% < C_7, 99.87% C_7 – C_{12}, and 0% > C_{12} hydrocarbon liquid fraction. While in 120 minutes reaction time produced 1.15% < C_7, 72.34% C_7 – C_{12}, and 26.51% > C_{12} hydrocarbon liquid fraction. It clearly seen that with an increase in reaction time, the formation of long chain hydrocarbon liquid fractions (> C_{12}) was preferred. The production of > C_{12} fractions increased by 26.51% as the reaction went from 60 minutes to 120 minutes.

The component of PS catalytic cracking product at reaction time 60 and 90 minutes was given in Figure 9. The major product of PS catalytic cracking with 60 minutes of exposure time were α-methyl styrene, benzocyclobutane, ethyl benzene, cumene, and toluene. Polystyrene undergoes two main reaction, a stepwise de-polymerization and polymer decomposition into oligomers followed by their consecutive cracking. Acid-catalyzed cracking mechanism could be categorized into carbenium nature. The most favorable reaction pathway included the attack of proton which associated with a Bronsted acidic site to the aromatic ring of PS since its phenyl group side was reactive enough toward electrophilic reagent. The carbocation further experienced β-scission followed by inter/intramolecular hydrogen transfer, resulting different products such as benzene, ethylbenzene, cumene, etc [16].

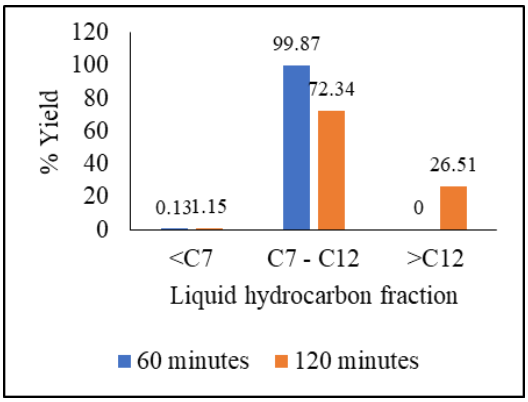

Figure 8 Distribution of liquid hydrocarbon fraction resulting from PS catalytic cracking for reaction time (a). 60 minutes (b). 120 minutes

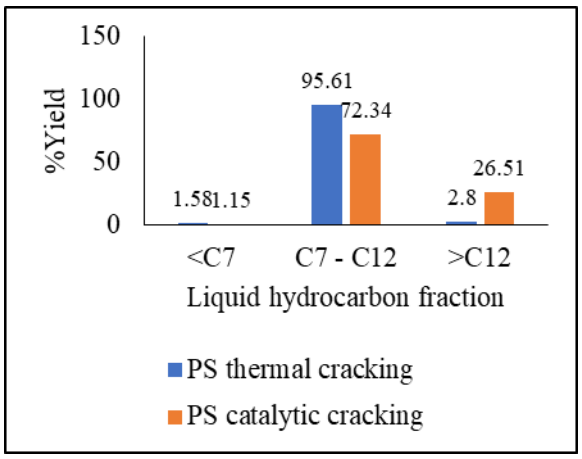

Figure 9 Distribution of liquid hydrocarbon fraction resulting from PS catalytic and thermal cracking for 120 minutes of reaction time

Similar PS degradation mechanism over acidic catalyst had been studied comprehensively [17]

Marczewski group's work revealed that the sequence of styrene dimers second reaction began from the attack of Brønsted acid sites on aromatic ring. The resulting carbenium ion underwent dealkylation and gave benzene and alkenylaromatic cation. The latter compound either reacts with a hydride anion gives phenylbutene or to phenylbutadiene, the coke precursor after proton detachment. Phenylbutene further experienced protonation either in

aromatic ring which results in dealkylation or in the aliphatic chain which initiates further transformation. It was found that two main reactions occur: internal cyclization and side chain cracking. The former reaction results in indane and naphthalene derivatives while the latter produces toluene, ethylbenzene and styrene. Moreover, the proposed reaction mechanism of PS cracking over Al-MCM-41-ceramis in the present study was depicted in Figure 11.

Increase in reaction time into 120 minute caused the formation of styrene dimers which contributed toward the enrichment of long chain hydrocarbon fractions (>C_{12}). It was due to the re-polymerization process of α-methylstyrene. This reaction mechanism was supported by the fact that the amount of α-methylstyrene as the major product in shorter reaction time (60 minutes) reduced by 52.26% after 120 minute reaction proceeded and lead to the formation of styrene dimer. Styrene dimer formed including diphenylmethane, diphenylethane, diphenylpropane, 1,3-diphenylbuthene, 1,3-diphenylbuthane, and 1,4-diphenyl-1,3-butadiene which identified from GC-MS analysis.

Similar PS degradation mechanism over acidic catalyst had been studied comprehensively [17]. Marczewski group's work revealed that the sequence of styrene dimers second reaction began from the attack of Brønsted acid sites on aromatic ring. The resulting carbenium ion underwent dealkylation and gave benzene and alkenylaromatic cation. The latter compound either reacts with a hydride anion gives phenylbutene or to phenylbutadiene, the coke precursor after proton detachment. Phenylbutene further experienced protonation either in aromatic ring which results in dealkylation or in the aliphatic chain which initiates further transformation. It was found that two main reactions occur: internal cyclization and side chain cracking. The former reaction results in indane and naphthalene derivatives while the latter produces toluene, ethylbenzene and styrene. Moreover, the proposed reaction mechanism of PS cracking over Al-MCM-41-ceramis in the present study was depicted in Figure 11.

Increase in reaction time into 120 minute caused the formation of styrene dimers which contributed toward the enrichment of long chain hydrocarbon fractions (>C_{12}). It was due to the re-polymerization process of α-methylstyrene. This reaction mechanism was supported by the fact that the amount of α-methylstyrene as the major product in shorter reaction time (60 minutes) reduced by 52.26% after 120 minute reaction proceeded and lead to the formation of styrene dimer. Styrene dimer formed including diphenylmethane, diphenylethane, diphenylpropane, 1,3-diphenylbuthene, 1,3-diphenylbuthane, and 1,4-diphenyl-1,3-butadiene which identified from GC-MS analysis.

3.3. Performance of Fuel Blend

The percentage of thermal efficiency of the fuel blend increases with increasing load (watts) on the gasoline engine as shown in Figure 11. At the low loading value (watts), CBC and CBT fuel blend variation have higher thermal efficiency compared to the mixture of premium and MTBE (CB sample) as a standard. However, at a maximum load of 2438 watts, the thermal efficiency of the CBC and CBT fuel mixture decreases and both have lower than premium values. CBC sample possess the highest thermal efficiency of 26.49% at 1843 watt loading values. At the same loading value, the thermal efficiency for CBT and CBC samples is 25.49% and 25.55% respectively. This is due to an increase in the long chain hydrocarbon fraction (> C12) of 26.51% from the catalytic cracking of polystyrene which has an effect on the density of CBC fuel blend variation. The thermal efficiency of the fuel blend is influenced by its heating value, density, and viscosity [22]. These three parameters greatly affect the amount of fuel which entering the carburettor and combustion process.

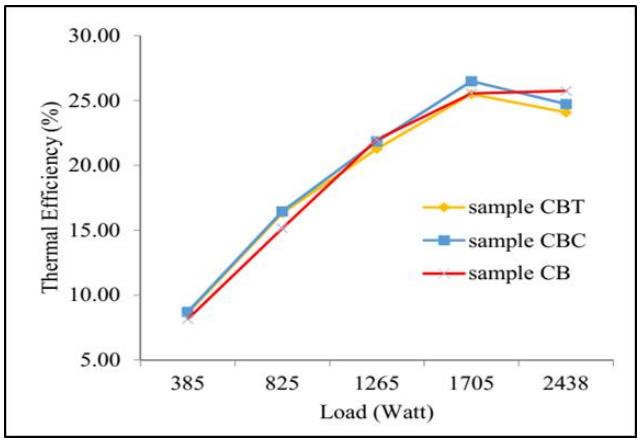

Figure 10 Thermal efficiency of fuel blend

4. Conclusion

Several conclusions can be drawn from the present study as follows. Modification of ceramic into Al-MCM-41 catalyst with mass ratio of Al-MCM-41 : ceramic 7:3 can increase the Si/Al ratio up to 45% without changing the hexagonal mesoporous structural properties of Al-MCM-41. Reaction time is one of the most important parameters that influence the selectivity of hydrocarbon liquid fraction in catalytic cracking process of polystyrene. Increase in reaction time from 60 minutes to 90 minutes of PS cracking over Al-MCM-41-ceramic catalyst leads to the enrichment of long chain hydrocarbon fraction (> C_{12}) by 25.61% which associated with the formation of styrene dimer due to the re-polymerization reaction in a batch system. The major styrene dimer obtained from 120 minutes reaction time including diphenylpropane, 1,3-diphenylbutene, and 1,3-diphenylbutane. Characteristics of liquid fuel blends produced are in accordance with SNI 06-3506-1994 with density value @ 15°C of 0.7405 g/cm^3, flash point of < -50°C, calorific value of 9642.42 kcal/kg, and octane number of 92.2. Performance testing on gasoline engines shows that the thermal efficiency percent of the fuel blend increases with increasing load (watts). The CBC fuel mixture has the highest thermal efficiency percent of 26.49% at the loading value of 1843 watts, where this value is greater than the mixture of premium-MTBE fuel which is equal to 25.55%.

Compliance with ethical standards

Acknowledgments

The authors gratefully acknowledge the funding support from ITS Local Research Grant for the Laboratory Research Scheme in 2022

Disclosure of conflict of interest

All of the authors declare that they have all participated in the design, execution, and analysis of the paper, and that they have approved the final version. Additionally, there are no conflicts of interest in connection with this paper, and the material described is not under publication or consideration for publication elsewhere.

References

[1] Aljabri N M, Lai Z, Hadjichristidis N and Huang K.-W., (2017) Renewable aromatics from the degradation of polystyrene under mild conditions, J. Saudi Chem. Soc., 21 983–89 https://doi.org/10.1016/j.jscs.2017.05.005

[2] Ojha D K and Vinu R., (2015) Resource recovery via catalytic fast pyrolysis of polystyrene using zeolites, J. Anal. Appl. Pyrolysis, 113 349–59 https://doi.org/10.1016/j.jaap.2015.02.024

[3] Fuentes-Ordóñez E G, Salbidegoitia J A, Ayastuy J L,Gutiérrez-Ortiz M A, González-Marcos M P and González-Velasco J R., (2014) High external surface Pt/zeolite catalysts for improving polystyrene hydrocracking, Catal. Today, 227 163–170 DOI:10.1016/j.cattod.2013.09.004.

[4] Miskolczi N, Bartha L and Deák G., (2006) Thermal degradation of polyethylene and polystyrene from the packaging industry over different catalysts into fuel-like feed stocks, Polym. Degrad. Stab., 91 517–26

[5] Tiwary P and Guria C., (2010) Effect of Metal Oxide Catalysts on Degradation of Waste Polystyrene in Hydrogen at Elevated Temperature and Pressure in Benzene Solution, J. Polym. Environ., 18 298–307

[6] Audisio G, Bertini F, Beltrame P L and Carniti P., (1990) Catalytic degradation of polymers: Part III—Degradation of polystyrene, Polym. Degrad. Stab., 29 191–200

[7] Juwono H, Triyono T, Sutarno S, Wahyuni E T, Ulfin I and Kurniawan F., (2017) Production of hydrocarbon (C7-C20) from hydrocracking of fatty acid methyl esters on Pd/Al-MCM-41 catalyst., Bull. Chem. React. Eng. Catal., 12 337–42

[8] Juwono H, Fauziah L, Uyun I Q, Alfian R, Suprapto, Ni'mah Y L and Ulfin I., (2018) Catalytic convertion of Al-MCM-41-ceramic on hidrocarbon (C8 – C12) liquid fuel synthesis from polypropylene plastic waste, AIP Conf. Proc. (Surabaya, Indonesia), vol 2049 p 020080.

[9] Juwono H, Triyono T, Sutarno S and Wahyuni E T., (2013) The influence of Pd impregnation into Al-MCM-41 on the characters and activity for biogasoline production by catalytic hydrocracking of FAMEs from nyamplung seed oil (Calophyllum Inophyllum), Indones. J. Chem., 13 171–75

[10] Juwono H, Triyono T, Sutarno S, Wahyuni E T, Ulfin I and Kurniawan F., (2017) Production of Biodiesel from Seed Oil of Nyamplung (Calophyllum inophyllum) by Al-MCM-41 and Its Performance in Diesel Engine, Indones. J. Chem., 17 316–21

[11] Juwono H, Nugroho K A, Alfian R, Ni'mah Y L, Sugiarso D and Harmami, (2019) New generation biofuel from polypropylene plastic waste with co-reactant waste cooking oil and its characteristic performance, J. Phys. Conf. Ser., 1156 012013

[12] Savidha R and Pandurangan A., (2004) Vapour phase isopropylation of phenol over zinc- and iron-containing Al-MCM-41 molecular sieves, Appl. Catal. Gen., 262 1–11

[13] Kang F, Wang Q and Xiang S., (2005) Synthesis of mesoporous Al-MCM-41 materials using metakaolin as aluminum source, Mater. Lett., 59 1426–29

[14] Kalargaris I, Tian G and Gu S., (2018) Experimental characterisation of a diesel engine running on polypropylene oils produced at different pyrolysis temperatures, Fuel, 211 797–803

[15] La-Salvia N, Lovón-Quintana J J and Valença G P., (2015) Vapor-phase catalytic conversion of ethanol into 1,3-butadiene on Cr-Ba/MCM-41 catalysts, Braz. J. Chem. Eng., 32 489–500

[16] Houshmand D, Roozbehani B and Badakhshan A., (2013) Thermal and catalytic degradation of polystyrene with a novel catalyst, Int. J. Sci. Emerging Tech., 5 234–38

[17] Marczewski M, Kamińska E, Marczewska H, Godek M, Rokicki G and Sokołowski J., (2013) Catalytic decomposition of polystyrene. The role of acid and basic active centers, Appl. Catal. B Environ., 129 236–246